

The Effect of Demagnetisation on the Susceptibility of Single-Domain Particles

Mathias Zambach,¹ Miriam Varón,¹ Mads R. Almind,¹ Matti Knaapila,^{1,2} Ziwei Ouyang,³ Marco Beleggia,^{4,5} and Cathrine Frandsen¹

¹*DTU Physics, Technical University of Denmark, 2800 Kgs. Lyngby, Denmark*

²*Department of Physics, Norwegian University of Science and Technology, 7491 Trondheim, Norway*

³*DTU Electro, Technical University of Denmark, 2800 Kgs. Lyngby, Denmark*

⁴*Department of Physics, University of Modena and Reggio Emilia, 41125 Modena, Italy*

⁵*DTU Nanolab, Technical University of Denmark, 2800 Kgs. Lyngby, Denmark*

(*Electronic mail: fracca@fysik.dtu.dk)

(Dated: 21 July 2025)

According to the classical laws of magnetism, the shape of magnetically soft objects limits the effective susceptibility. For example, spherical soft magnets cannot display an effective susceptibility larger than 3. Although true for macroscopic multi-domain magnetic materials, we explain why magnetic nanoparticles in a single-domain state do not suffer from this limitation. We show that the differences between demagnetisation factors along principal axes are relevant and can influence susceptibility for single-domain particles, but do not limit the susceptibility as in the case for multi-domain particles. We validate this result experimentally on spherical nanoparticles with varying diameter (8 to 150 nm) and varying volume fraction (0.1 to 47 vol%). In agreement with our predictions, we measure susceptibilities largely above 3, in fact up to more than 250, for single-domain particles. Moreover, contrary to an existing model, we find that the susceptibility of non-interacting single-domain particles in a non-magnetic matrix scales simply linearly with the volume fraction of particles.

Magnetic susceptibility - the change of magnetization upon a change in applied field - is one of the main material parameters to consider when designing magnetic components. Some materials have very high bulk susceptibilities, for instance iron has it above 1000. However, according to the shape of the magnet, the demagnetizing field diverging from the magnetic poles can limit the effective susceptibility to a purely geometric effect even for highly susceptible materials.

It is a well-known text book result that the effective susceptibility, $\chi_{p,\text{eff}}$, of a (multi-domain) particle is given as

$$\chi_{p,\text{eff}} = \frac{1}{N + 1/\chi_p}, \quad (1)$$

where N is the demagnetisation factor of the particle along the applied field direction and χ_p is the intrinsic susceptibility of the particle. The effective susceptibility for magnetically soft materials is therefore at most $1/N$, or 3 in case of magnetic spheres where $N = 1/3$. Consequently, large effective susceptibilities can only be achieved with particles elongated and aligned along the applied field direction. Eq. (1) is derived implicitly for multi-domain magnets. We question whether it holds for single-domain particles: as these are always magnetically saturated their susceptibility may not be limited by demagnetization effects in the same way. Along these lines, Skomski et al. (2010)¹ found unusual demagnetization effects in magnetization processes of nanoscale spheres (due to coherent magnetization rotation), but did not explore it further.

For ensembles of magnetic particles, the demagnetization correction is more complex due to the combined contributions from the shape of the individual particles, their interactions, and the shape of the sample²⁻⁸. For systems of spherical (multi-domain) particles, a global demagnetisation factor that depends on particle volume fraction, f , and on the demagnetization

factors of both spherical particles $N = 1/3$ and sample shape N_s , has been proposed^{2-5,7,8}

$$N_c = \frac{1}{3} + f \left(N_s - \frac{1}{3} \right), \quad (2)$$

While this model may apply to ensembles of multi-domain particles⁵, it is uncertain if it is valid in case of single-domain particles⁵, especially if Eq. (1) does not hold for single-domain particles. With Eq. (2), the effective ensemble susceptibility will be at most ≈ 11.5 (assuming $f = 0.74$ for close-packed spheres and $N_s = 0$). Susceptibility measurements on systems of single-domain nanoparticles of Fe^{6,9}, FeNi¹⁰⁻¹³, FeCo^{14,15}, and ferrites^{16,17} indicate that spherical single-domain particles may not be limited by demagnetisation effects in the same way as multi-domain soft spherical magnets, although this is not discussed in these references.

Designing high-susceptibility materials is of great interest. For example, new magnetic composite materials containing single-domain magnetic particles are being investigated for sensors¹⁸⁻²⁰ and for micro-inductor cores in power electronics^{6,9-12,14-17,21-27}. For these applications, it is crucial to understand the effective magnetic susceptibility of single-domain magnetic particles and composite materials containing them.

This letter takes a fundamental approach to clarify the underlying physics to the questions: i) is the susceptibility of single-domain particles limited by shape in the same way as for multi-domain particles? and ii) which demagnetization factor describes an ensemble of non-interacting spherical single-domain particles?

First, we note that the demagnetisation field in single-domain particles differs from the multi-domain case: the mag-

netization is saturated at all times. Hence, the magnitude of the demagnetisation field in single-domain particles does not increase due to an induced magnetisation with applied field as found for multi-domain particles. Instead, the demagnetisation field rotates with the saturated magnetisation according to the demagnetisation factors. This modifies the way that demagnetisation factors enters the effective susceptibility for single-domain particles compared to the case of multi-domain particles.

For both single-domain and multi-domain particles, the particle susceptibility tensor components, $\chi_{p,ij}$, and effective particle susceptibility, $\chi_{p,\text{eff}}$, can be written as

$$\chi_{p,ij} = \frac{\partial M_i}{\partial H_{ij}} \quad \text{and} \quad \chi_{p,\text{eff}} = \frac{\partial(\mathbf{M} \cdot \hat{\mathbf{H}})}{\partial H}. \quad (3)$$

Here, M_i is the component of the magnetisation in the i -direction, H_{ij} is the internal field strength of the particle in the j direction, H is the applied field amplitude, and $\hat{\mathbf{H}}$ is the applied field direction unit vector. For uniformly magnetised particles, the demagnetisation field can be described by the demagnetisation tensor components, N_{jk} , such that the internal field component becomes

$$H_{ij} = H_j + H_{d,j} = H_j - N_{jk}M_k. \quad (4)$$

In Eq.(4) and thereafter we assume summation over repeated indexes.

In the multi-domain case, the linear relationship is $M_j = \chi_p H_{ij}$. Thus, $\chi_{p,ij} = (\delta_{ij}/\chi_p + N_{ij})^{-1}$, such that the effective susceptibility for multi-domain particles is

$$\chi_{p,\text{eff}} = \frac{h_x^2}{N_{xx} + 1/\chi_p} + \frac{h_y^2}{N_{yy} + 1/\chi_p} + \frac{h_z^2}{N_{zz} + 1/\chi_p} \quad (5)$$

with $h_{x,y,z}$ being the direction cosines of the applied field, i.e. $\hat{\mathbf{H}} = (h_x, h_y, h_z)$. This expression is usually known in the format of Eq. (1), where N is the demagnetisation factor in the applied field direction. This is the expression showing that $\chi_{p,\text{eff}}$ is limited to 3 for spheres of soft magnetic materials.

In case of a single-domain (blocked) particle, the magnetic moment will, without applied field, be aligned to the easy axis. We set the z -axis along this direction so that without applied field $\hat{\mathbf{M}} = \hat{\mathbf{z}}$. The magnetostatic energy for a uniformly magnetised ellipsoid with saturation magnetisation M_s is

$$\frac{E}{K_d V} = (N_{xx}m_x^2 + N_{yy}m_y^2 + N_{zz}m_z^2) - \mathcal{H}(\hat{\mathbf{M}} \cdot \hat{\mathbf{H}}), \quad (6)$$

with $m_{x,y,z}$ being the directional cosines of the magnetisation, $\hat{\mathbf{M}} = (m_x, m_y, m_z)$, V being the particle volume, and $K_d = \mu_0 M_s^2 / 2$, and $\mathcal{H} = 2H/M_s$. In absence of an applied field, Eq. (6) can be set equal to the contribution from the magnetisation along the z -axis, i.e. $E/(K_d V) = N_{zz}$. Using that $m_z \approx 1$ for small fields, we can write

$$0 = (N_{xx} - N_{zz})m_x^2 + (N_{yy} - N_{zz})m_y^2 - 2\mathcal{H}(m_x h_x + m_y h_y + h_z). \quad (7)$$

From (7), we find the x and y components of the magnetisation by setting the energy gradients with respect to m_x and m_y to zero, obtaining

$$m_x = \frac{\mathcal{H} h_x}{N_{xx} - N_{zz}} \quad \text{and} \quad m_y = \frac{\mathcal{H} h_y}{N_{yy} - N_{zz}}. \quad (8)$$

By use of equation (3) the effective susceptibility for a blocked, single-domain particle when only considering shape anisotropy is then

$$\chi_{p,\text{eff}} = \frac{h_x^2}{N_{xx} - N_{zz}} + \frac{h_y^2}{N_{yy} - N_{zz}}. \quad (9)$$

Noticeably, this shows that the effective susceptibility for single-domain particles depends on the *difference* in demagnetisation factors along the principal axes of the given shape.

Along the same lines as above we find, that the susceptibility perpendicular to the the easy axis of a prolate particle, where the shape anisotropy easy axis is set parallel to the magneto-crystalline uniaxial anisotropy easy axis, is

$$\chi_{p,\text{eff}} = \frac{\chi'_p}{1 + \chi'_p(N_{ii} - N_{jj})}, \quad (10)$$

with the perpendicular Stoner-Wohlfarth susceptibility $\chi'_p = \frac{\mu_0 M_s^2}{2K_u}$ and the difference between demag factors along the principal axis of the spheroid $N_{ii} - N_{jj}$.

Thus, the shape anisotropy does not limit the effective susceptibility to $1/N$ as it does for the multi-domain case. In detail, Eqs. (9) and (10) establish that for ellipsoidal single-domain particles, the susceptibility will only be limited by $1/(N_{ii} - N_{jj})$ due to demagnetisation effects, which has no upper limit, and for spherical single-domain particles, where $N_{xx} = N_{yy} = N_{zz} = 1/3$, $\chi_{p,\text{eff}}$ is not 3, but diverges towards the particle susceptibility from other anisotropies. Eq. (9) reveals also that, in clear contrast to the multi-domain case, spherical single-domain particles achieve the highest susceptibility.

For sufficiently small single-domain particles, thermal energy can induce superparamagnetism. The particle magnetization, while it remains single-domain, reverses at time scales shorter than the observation time. The characteristic timescale, τ , for relaxation between easy directions, depends on the anisotropy energy relative to thermal energy. The time-averaged magnetisation and susceptibility can be found as for a paramagnetic ion (see, e.g.,^{26,28}).

To clarify the effect of demagnetisation on the superparamagnetic particle susceptibility we write the demagnetisation energy of a uniformly magnetised single-domain spheroid particle as

$$E_{H_d} = -\frac{\mu_0}{2} \int_V \mathbf{M}_s \cdot \mathbf{H}_d dV = K_{sh} V \sin^2 \Theta, \quad (11)$$

with the shape anisotropy constant $K_{sh} = K_d(N_{ii} - N_{jj})$. Here N_{ii} and N_{jj} are the demagnetisation factors along the principal spheroid axes. K_{sh} is positive (/negative) for oblate (/prolate) spheroids, respectively, and Θ is the angle between the magnetic moment and the longer (/shorter) principal spheroid axis.

We find the superparamagnetic particle susceptibility to be

$$\chi_{\text{spm}}(\theta_H) = \frac{\epsilon_M}{2} [\sin^2 \theta_H + R'/R (3 \cos^2 \theta_H - 1)] \quad (12)$$

with

$$R' = \int_0^1 x^2 \exp(\epsilon_k x^2) dx \quad \text{and} \quad R = \int_0^1 \exp(\epsilon_k x^2) dx. \quad (13)$$

for a non-interacting, uniaxial anisotropy particle with the applied field at an angle θ_H to the anisotropy axis. Here, the energy ratios used are

$$\epsilon_k = \frac{KV}{k_B T}, \quad \text{and} \quad \epsilon_M = \frac{\mu_0 V M_s^2}{k_B T}, \quad (14)$$

with K being the effective anisotropy, in our case $K = K_{\text{sh}}$. If the length difference between the axes is larger than 5-10%, then shape anisotropy dominates over magneto-crystalline anisotropy for most soft magnetic particle materials. For uniaxial anisotropy particles the susceptibility ranges from ϵ_M to 0 in case of large anisotropy ($\epsilon_k \gg 1$) as R'/R goes towards 1. For low anisotropy ($\epsilon_k \ll 1$) the limit of R'/R is $1/3$ and the susceptibility of the uniaxial anisotropy particle goes towards the random case value $\epsilon_M/3$ for all θ_H .

From above it is clear that the susceptibility is $\epsilon_M/3$ for a spherical particle, i.e. $K_{\text{sh}} = 0$, and therefore, neither in the superparamagnetic single-domain case, is the susceptibility limited to 3 by demagnetisation effects. If we increase the shape anisotropy we observe that demagnetisation results in slightly larger susceptibility for fields along the long axis and slightly lower susceptibility for fields perpendicular to the long axis. Hence, demagnetisation in superparamagnetic particles acts in similar way as for the blocked case: the differences in demagnetisation factors along primary axes in the particle are of importance. However, susceptibility is further enhanced in some cases due to the anisotropy.

For non-interacting, randomly oriented superparamagnetic particles, one can average over all possible directions for Eq. (12) and thus recover the well known per particle susceptibility

$$\langle \chi_{\text{spm}} \rangle = \frac{\epsilon_M}{3} = \frac{\mu_0 V M_s^2}{3 k_B T}. \quad (15)$$

Eq. (15) reveals that shape anisotropy is washed out in random ensembles of superparamagnetic particles, as all individual contributions to the susceptibility are averaged by the randomness of the particle axis with respect to the applied field direction.

To test our predictions that effective particle susceptibilities above $1/N$ are possible for single-domain particles, we investigated a series of samples containing spherical, fcc Co particles with sizes (mean diameters) ranging between 8 and 150 nm on porous Al_2O_3 support. Particle sizes and distributions were determined by Transmission Electron Microscopy (TEM). Magnetic properties were measured at 200 °C under reducing conditions (2.4% H_2 in Ar) by vibrating sample magnetometry (VSM), with the exception of the sample with 8 nm

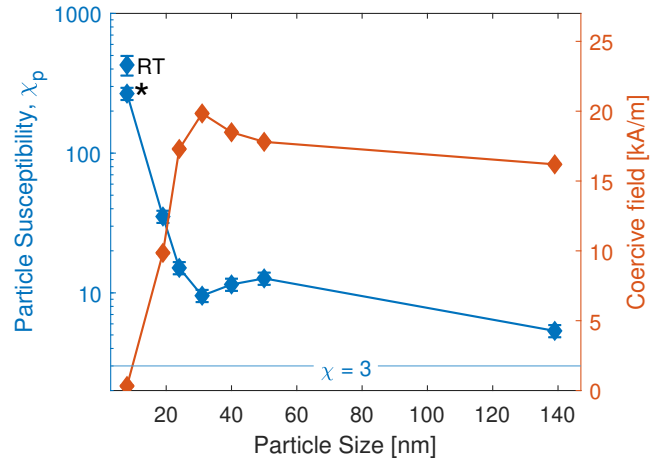


FIG. 1. Susceptibility and coercive field of fcc Co particles of varying size on Al_2O_3 support, measured at 200 °C after full reduction at 900 °C. Major/Minor loops measured at applied fields up to 1 T/10 mT. Particle sizes were found by TEM after magnetic characterisation. 8 nm particles were measured at room-temperature (RT) and χ was corrected as $1/T$ to 200 °C (indicated by *).

Co particles that was measured at room temperature, while under same gas conditions, and its particle susceptibility was $1/T$ -corrected to 200 °C. For all samples, the Co had been fully reduced in their VSM holder at 900 °C prior to the measurements. The Co particles showed saturation magnetisation of 1448 kA/m. Particle susceptibility were then calculated from demagnetisation corrected sample susceptibility and volume fraction of particles.

Figure 1 shows the measured particle susceptibility and coercivity for Co particles vs. size at 200 °C. It is seen that particle susceptibility for the single domain particles (8-50 nm diameter) are above 9, proving that demagnetisation does not limit particle susceptibility to 3. The particle susceptibility for the smallest particles is even above 250 at 200 °C (400 at room-temperature), with a small coercivity, indicating superparamagnetism. The peak in coercive field indicates that that particles with diameters between 30-60 nm are blocked. Co below 80 nm in diameter has been found to be single domain²⁹. It is noted that for the larger particles (140 nm diameter) the susceptibility does not drop to 3. Most likely, these particles are pseudo single-domain i.e. only support few domains, and not fully fitting for the multi-domain case described by equation (1). In all, the measurements of Fig. 1 support that particle susceptibilities above 3 are possible for single-domain particles in both the blocked and superparamagnetic state.

Having derived the effect of demagnetisation on single particle susceptibility, we turn to the topic of nanocomposite susceptibility for materials containing single-domain magnetic particles in a non-magnetic matrix. The most straightforward description would be a linear model²⁸, where the intrinsic susceptibility of the composites, χ_{nc} , is simply the particle volume fraction, f , times the particle susceptibility

$$\chi_{\text{nc}} = f \chi_p. \quad (16)$$

This model is often used implicitly for ferromagnetic fluids or other dilute particle systems^{28,30,31}. It seems readily adaptable to describe the susceptibility of a system of isolated, single-domain particles where the particle susceptibility is not limited to $1/N$, but the validity of the model has not yet been systematically investigated for denser particle systems. Specifically, in cases where inter-particle interactions prevail, composite susceptibility may deviate from linear.

Demagnetization correction for nanocomposite sample shape should still be performed, even if Eq. (16) are valid. That is Eq. (1) is applied to χ_{nc} of Eq. (16) with the demagnetisation factor $N = N_s$ in the applied field direction as

$$\chi_{nc} = \frac{1}{1/\chi_{nc, eff} - N_s}. \quad (17)$$

If the model implied by Eq. (16) (and Eq. (17)) is valid for nanocomposites, then it precludes Eq. (2), which corrects for both particle and sample shapes. Normile et al.³² have used the demagnetization factor from Eq. (2) to derive the intrinsic susceptibility of 8 nm maghemite particles in dense assemblies. However, they got large discrepancies in intrinsic susceptibilities (5 vs. 15) for similar particles in thin and thick disk samples and similar volume fraction (50 vs 59 vol%), suggesting that Eq. (2) may not be suitable for nanocomposites.

In order to test if Eq. 16 is applicable to systems of isolated single-domain particles we prepared and investigated a series of nanocomposites containing varying fraction of spherical γ -Fe₂O₃ (maghemite) particles of 11 ± 3 nm diameter fixed in a poly-vinyl alcohol polymer matrix. The nanocomposite samples were cast as discs with a thickness of 100-400 μ m and diameter of 6 mm. Small-angle neutron scattering confirmed near-spherical particle shape and particle size distributions obtained from TEM, as well as absence of aggregation in the polymer matrix. Detailed description and characterisation of the synthesised nanocomposites is presented elsewhere²⁷.

We measured the nanocomposites by VSM with sample disc planes parallel to the applied field. All nanocomposite samples showed Langevin behaviour typical for superparamagnetic nanoparticles fitting with distributions similar to the TEM results. No detectable hysteresis was found with coercive fields below 4 ± 8 A/m at 298 K. Particle saturation magnetisation of $M_s = 303$ kA/m was found from liquid samples for which iron content had been quantified by inductively coupled plasma mass spectrometry³³. Magnetic particle content in the composites was calculated by use of the particle saturation magnetisation, matrix density of 1 g/cm³, and maghemite density of 4.88 g/cm³.

Figure 2 shows resulting nanocomposite susceptibilities obtained from the VSM measurements. Here, $\chi_{nc, eff}$ (open circles) is given as-measured, and χ_{nc} (solid squares) is demagnetisation corrected for nanocomposite sample shape (disk/flat cylinder), cf. Eq. (17). The used sample shape demagnetisation factors are calculated according to Ref.³⁴. The relatively smaller $\chi_{nc, eff}$ of the sample with 44 vol% is due to its thicker disk size, and, when demagnetisation corrected for the sample shape, the nanocomposite material follows a linear trend for χ_{nc} in correspondence with Eq. 16. The theoretic

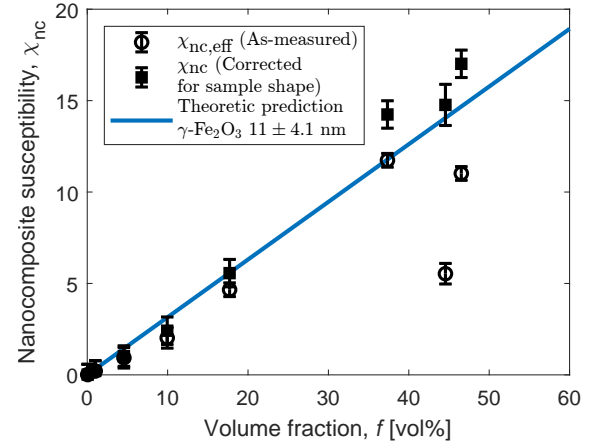


FIG. 2. Measured susceptibility of nanocomposites containing randomly oriented 11 ± 3 nm diameter γ -Fe₂O₃ particles as function of volume fraction of particles and theoretic prediction. $\chi_{nc, eff}$ (open circles) is the measured nanocomposite susceptibility and χ_{nc} (solid squares) is the measured susceptibility corrected for the sample shape. Theoretic prediction based on Eqs. (15)-(16), with log-normal size distribution, $M_s = 303$ kA/m, and $T = 298$ K.

prediction (full line) in Fig. 2, is based on Eqs. (15) and (16), log-normally distributed maghemite particles with $M_s = 303$ kA/m²⁷ and a mean diameter of 11 ± 4.1 nm. We note that the sample shape demagnetization corrected susceptibilities χ_{nc} are in agreement with our predictions, despite a slightly larger log-normal distribution width than derived from TEM (4.1 nm vs 3 nm), but this variation is within the experimental uncertainty of the TEM data.

For all the nanocomposites in Fig. 2, the corresponding intrinsic particle susceptibility χ_p (cf. Eq. (16)) is consistently around 25. First, this confirms that χ_p is not limited to 3 for spherical nanoparticles. Second, it exemplifies that Eq. (2) cannot hold, as such consistency in χ_p is not obtainable by Eq. (2). Moreover, the high susceptibilities expose experimentally that the demagnetisation factor in Eq. (2), which correct for both particle shape and sample shape, is not applicable to nanoparticle systems. The measured nanocomposite susceptibilities of 11.0 - 11.7 (Fig. 2), are too high to be explained by the demagnetization factor in Eq. (2): $\chi_{nc, eff}$ could maximally be 5.6 for 46 vol% of spherical nanoparticles, if using the demagnetisation factor in Eq. (2). Additionally, if the here measured nanocomposite susceptibilities of 4.7-11.7 for the 17-46 vol% samples (Fig. 2) were demagnetisation corrected for both particle shape and sample shape, as in Eqs. (1)-(2), then meaningless negative intrinsic susceptibilities, χ_{nc} , of -5.1 to -9.4, are obtained, equivalent to overskewed hysteresis loops¹.

Overall, this shows that the demagnetisation factor given in Eq. (2), which may apply to composites of multi-domain particles⁵, is not applicable to systems of isolated single-domain nanoparticles. $\chi_{nc, eff}$ should be corrected for sample shape, but not spherical particle shape. Hence, in order to derive χ_{nc} from experimental measurements on nanocomposites containing isolated, single-domain particles, we suggest following procedure: for a specific sample (e.g. a thin disc of

nanocomposite), the effective susceptibility is measured in a certain direction and the measurement is demagnetisation corrected for the sample shape only.

In general, influences of inter-particle interactions are a potential concern for the design of dense nanoparticle composites. Interactions have been reported in literature to either increase or decrease particle susceptibility^{6,28,35,36}. In our test samples containing up to 46 vol% 11 ± 4.1 nm γ -Fe₂O₃ particles, we do not observe clear signs of inter-particle interactions, cf. Eq. (16) applies. We estimate the dipolar interaction between particle pairs in our system (1-46 vol% 11 ± 3 nm γ -Fe₂O₃) to be on the scale of $7\text{--}70 \times 10^{-22}$ J, using $\mu_0 m^2 / (4\pi r_{cc}^3)$, where r_{cc} is the mean center-center distance of the particles. This estimate does not take into account the fluctuating nature of the particle magnetisation and that one particle has several neighbours which may lead to increased/decreased interaction fields. When comparing to the anisotropy barrier (KV) which is in the range of 170×10^{-22} J when using $K \approx 25$ kJ/m³, the found interaction energy scale for our system may be insignificant. This is also in agreement with the simulations in³⁷ for similar ϵ_k and ϵ_M .

In conclusion, we have explained why the effective single-domain particle susceptibility is not limited by demagnetisation, neither for superparamagnetic nor for blocked single-domain particles. The difference between demagnetisation factors along the applied field direction and the particle easy axis is of importance, but enters mainly like an extra (shape) anisotropy and for spherical particles the susceptibility is not affected by particle demagnetisation. It is noticeably that near-spherical shape is the most favourable for obtaining a high effective susceptibility in single-domain particles, in contrast to multi-domain cases. We have validated experimentally the improvement over the classical susceptibility limit by two nanocomposite systems: spherical fcc Co particles of different sizes verify that neither superparamagnetic nor blocked single-domain particles have a particle susceptibility limited by demagnetisation (i.e. $\chi_p \gg 3$); spherical superparamagnetic γ -Fe₂O₃ particles in different volume fractions confirm that the conventional particle demagnetisation limit does not apply, and conclude that the nanocomposite susceptibility depends linearly on particle volume fraction for non-interacting nanoparticles. Consequently, Eq. 2 does not apply to single-domain particles. The presented results are important for the design of new soft magnetic materials.

ACKNOWLEDGMENTS

The authors thank Ron B. Goldfarb for providing helpful feedback to a previous version of this manuscript and the Independent Research Fund Denmark for financial support (project HiFMag, grant number 9041-00231A).

DATA AVAILABILITY STATEMENT

The data that support the findings of this study are available from the corresponding author upon reasonable request.

- ¹R. Skomski, Y. Liu, J. E. Shield, G. C. Hadjipanayis, and D. J. Sellmyer, "Permanent magnetism of dense-packed nanostructures," *Journal of Applied Physics* **107**, 09A739 (2010), https://pubs.aip.org/aip/jap/article-pdf/doi/10.1063/1.3337657/13561491/09a739_1_online.pdf.
- ²G. Breit, "Calculations of the effective permeability and dielectric constant of a powder," *Proceedings of the Koninklijke Akademie Van Wetenschappen Te Amsterdam* **25**, 293–308 (1923).
- ³B. Bleaney and R. Hull, "The effective susceptibility of a paramagnetic powder," *Proceedings of the Royal Society of London Series A-mathematical and Physical Sciences* **178**, 0086–0092 (1941).
- ⁴R. Skomski, G. C. Hadjipanayis, and D. J. Sellmyer, "Effective Demagnetizing Factors of Complicated Particle Mixtures," *IEEE Transactions on Magnetics* **43**, 2956–2958 (2007).
- ⁵R. Bjørk and C. R. Bahl, "Demagnetization factor for a powder of randomly packed spherical particles," *Applied Physics Letters* **103**, 102403 (2013).
- ⁶M. Kin, H. Kura, and T. Ogawa, "Core loss and magnetic susceptibility of superparamagnetic Fe nanoparticle assembly," *Aip Advances* **6**, 125013 (2016).
- ⁷F. H. Sánchez, P. Mendoza Zélis, M. L. Arciniegas, G. A. Pasquevich, and M. B. Fernández van Raap, "Dipolar interaction and demagnetizing effects in magnetic nanoparticle dispersions: Introducing the mean-field interacting superparamagnet model," *Phys. Rev. B* **95**, 134421 (2017).
- ⁸S. M. McCann, J. Leach, S. M. Reddy, and T. Mercer, "Methods of investigating the demagnetization factors within assemblies of superparamagnetic nanoparticles," *Aip Advances* **12**, 075212 (2022).
- ⁹H. Kura, T. Ogawa, R. Tate, K. Hata, and M. Takahashi, "Size effect of Fe nanoparticles on the high-frequency dynamics of highly dense self-organized assemblies," *Journal of Applied Physics* **111**, 07B517 (2012).
- ¹⁰K. Yatsugi, T. Ishizaki, K. Akedo, and M. Yamauchi, "Composition-controlled synthesis of solid-solution Fe-Ni nanoalloys and their application in screen-printed magnetic films," *Journal of Nanoparticle Research* **21**, 60 (2019).
- ¹¹X. Lu, G. Liang, Q. Sun, and C. Yang, "High-frequency magnetic properties of FeNi₃-SiO₂ nanocomposite synthesized by a facile chemical method," *Journal of Alloys and Compounds* **509**, 5079–5083 (2011).
- ¹²W. Liu, W. Zhong, H. Y. Jiang, N. J. Tang, X. L. Wu, and W. Y. Du, "Synthesis and magnetic properties of FeNi₃/Al₂O₃ core-shell nanocomposites," *European Physical Journal B* **46**, 471–474 (2005).
- ¹³G. V. Williams, J. Kennedy, P. P. Murmu, S. Rubanov, and S. V. Chong, "The effect of different Fe concentrations on the structural and magnetic properties of near surface superparamagnetic Ni_{1-x}Fe_x nanoparticles in SiO₂ made by dual low energy ion implantation," *Journal of Magnetism and Magnetic Materials* **473**, 125–130 (2019).
- ¹⁴H. Kura, K. Hata, T. Oikawa, M. Takahashi, and T. Ogawa, "Effect of induced uniaxial magnetic anisotropy on ferromagnetic resonance frequency of Fe-Co alloy nanoparticle/polystyrene nanocomposite," *Scripta Materialia* **76**, 65–68 (2014).
- ¹⁵B. Yang, Y. Wu, X. Li, and R. Yu, "Chemical synthesis of high-stable amorphous FeCo nanoalloys with good magnetic properties," *Nanomaterials* **8**, 154 (2018).
- ¹⁶H. Yun, X. Liu, T. Paik, D. Palanisamy, J. Kim, W. D. Vogel, A. J. Viescas, J. Chen, G. C. Papaefthymiou, J. M. Kikkawa, M. G. Allen, and C. B. Murray, "Size- and composition-dependent radio frequency magnetic permeability of iron oxide nanocrystals," *Acs Nano* **8**, 12323–12337 (2014).
- ¹⁷H. Yun, J. Kim, T. Paik, L. Meng, P. S. Jo, J. M. Kikkawa, C. R. Kagan, M. G. Allen, and C. B. Murray, "Alternate current magnetic property characterization of nonstoichiometric zinc ferrite nanocrystals for inductor fabrication via a solution based process," *Journal of Applied Physics* **119**, 113901 (2016).
- ¹⁸S. Bedanta, T. Eimüller, W. Kleemann, J. Rhensius, F. Stromberg, E. Amaladass, S. Cardoso, and P. P. Freitas, "Overcoming the Dipolar Disorder in Dense CoFe Nanoparticle Ensembles: Superferromagnetism," *Phys. Rev. Lett.* **98**, 176601 (2007).
- ¹⁹D. Moretti, P. P. Sharma, D. Petti, E. Albisetti, R. Bertacco, P. Baldelli, and F. Benfenati, "Magnetic Tunnel Junction Based Chip to Detect the Mag-

- netic Field of Neuronal Signals: A Platform for In Vitro Studies,” *Proceedings* **1**, 735 (2017).
- ²⁰N. Peserico, P. Pratim Sharma, A. Belloni, F. Damin, M. Chiari, R. Bertacco, and A. Melloni, “Enhancement of integrated photonic biosensing by magnetic controlled nano-particles,” *Progress in Biomedical Optics and Imaging - Proceedings of Spie* **10506**, 105060N (2018).
 - ²¹C. R. Sullivan, D. V. Harburg, J. Qiu, C. G. Levey, and D. Yao, “Integrating magnetics for on-chip power: A perspective,” *IEEE Transactions on Power Electronics* **28**, 4342–4353 (2013).
 - ²²C. Garnero, M. Lepasent, C. Garcia-Marcelot, Y. Shin, C. Meny, P. Farger, B. Warot-Fonrose, R. Arenal, G. Viau, K. Soulantica, P. Fau, P. Poveda, L. M. Lacroix, and B. Chaudret, “Chemical ordering in bimetallic FeCo nanoparticles: From a direct chemical synthesis to application as efficient high-frequency magnetic material,” *Nano Letters* **19**, 1379–1386 (2019).
 - ²³D. Hasegawa, H. Yang, T. Ogawa, and M. Takahashi, “Challenge of ultra high frequency limit of permeability for magnetic nanoparticle assembly with organic polymer-Application of superparamagnetism,” *Journal of Magnetism and Magnetic Materials* **321**, 746–749 (2009).
 - ²⁴M. P. Rowe, S. Sullivan, R. D. Desautels, E. Skoropata, and J. Van Lierop, “Rational selection of superparamagnetic iron oxide/silica nanoparticles to create nanocomposite inductors,” *Journal of Materials Chemistry C* **3**, 9789–9793 (2015).
 - ²⁵B. N. Sanusi, M. Zambach, M. Varon, M. Beleggia, C. Frandsen, and Z. Ouyang, “Low Profile Superparamagnetic Inductor for Portable Electronics Power Management,” *IEEE Transactions On Power Electronics* [**Accepted**] (2025).
 - ²⁶M. Zambach, Z. Ouyang, M. Knaapila, M. Beleggia, and C. Frandsen, “Design of superparamagnetic nanoparticle-materials for high-frequency inductor cores,” (2024), arXiv:2308.13407 [cond-mat.mes-hall].
 - ²⁷M. Zambach, M. Varón, T. Veile, B. N. Sanusi, M. Knaapila, A. M. Jørgensen, L. Almásy, C. Johansson, Z. Ouyang, M. Beleggia, and C. Frandsen, “Printable High-susceptibility Nanocomposites of Superparamagnetic maghemite ($\gamma\text{-Fe}_2\text{O}_3$) Particles for Micro-inductor-core Applications,” [Preprint] (2025).
 - ²⁸E. A. Elfimova, A. O. Ivanov, and P. J. Camp, “Static magnetization of immobilized, weakly interacting, superparamagnetic nanoparticles,” *Nanoscale* **11**, 21834–21846 (2019).
 - ²⁹K. M. Krishnan, “Biomedical nanomagnetism: A spin through possibilities in imaging, diagnostics, and therapy,” *IEEE Transactions on Magnetics* **46**, 2523–2558 (2010).
 - ³⁰K. Bai, J. Casara, A. Nair-Kanneganti, A. Wahl, F. Carle, and E. Brown, “Effective magnetic susceptibility of suspensions of ferromagnetic particles,” *Journal of Applied Physics* **124**, 123901 (2018).
 - ³¹J. Carrey, B. Mehdaoui, and M. Respaud, “Simple models for dynamic hysteresis loop calculations of magnetic single-domain nanoparticles: Application to magnetic hyperthermia optimization,” *Journal of Applied Physics* **109**, 083921 (2011).
 - ³²P. S. Normile, M. S. Andersson, R. Mathieu, S. S. Lee, G. Singh, and J. A. De Toro, “Demagnetization effects in dense nanoparticle assemblies,” *Applied Physics Letters* **109**, 152404 (2016).
 - ³³R. Costo, D. Heinke, C. Grüttner, F. Westphal, M. P. Morales, S. Veintemillas-Verdaguer, and N. Gehrke, “Improving the reliability of the iron concentration quantification for iron oxide nanoparticle suspensions: a two-institutions study,” *Analytical and Bioanalytical Chemistry* **411**, 1895–1903 (2019).
 - ³⁴M. Beleggia, M. De Graef, Y. T. Millev, D. A. Goode, and G. Rowlands, “Demagnetization factors for elliptic cylinders,” *Journal of Physics D: Applied Physics* **38**, 3333–3342 (2005).
 - ³⁵R. W. Chantrell, N. Walmsley, J. Gore, and M. Maylin, “Calculations of the susceptibility of interacting superparamagnetic particles,” *Physical Review B - Condensed Matter and Materials Physics* **63**, 024410/1–14 (2001).
 - ³⁶N. A. Usov and O. N. Serebryakova, “Equilibrium properties of assembly of interacting superparamagnetic nanoparticles,” *Scientific Reports* **10**, 13677 (2020).
 - ³⁷F. L. Durhuus, T. H. v. B. Rix, M. A. Glód, M. Beleggia, and C. Frandsen, “Néel relaxation of magnetic nanoparticle clusters,” *IEEE Magnetics Letters*, 1–5 (2025).